Bisphosphine monoxides with *o*-phenylene backbones in Pt, Pd and Fe complexes

Nicola J. Farrer [a,b], Robert McDonald [c], Toria Piga [b], J. Scott McIndoe [b,*]

[a] *Department of Chemistry, The University of Cambridge, Lensfield Road, Cambridge CB2 1EW, UK*
[b] *Department of Chemistry, The University of Victoria, P.O. Box 3065, Victoria, BC, Canada V8W 3V6*
[c] *X-ray Crystallography Laboratory, Department of Chemistry, University of Alberta, Edmonton, AB, Canada T6G 2G2*

ARTICLE INFO

ABSTRACT

A new route to aromatic bisphosphine monoxides has been explored through *ortho*lithiation of triphenylphosphine oxide and subsequent reaction of the lithiated intermediate with a range of alkyl and aryl phosphine chlorides. Routes to the known bisphosphine monoxide (BMPO) (o-C_6H_4){P(O)Ph$_2$}PPh$_2$ (**2aO**) and a range of new BPMOs of the type $Ph_2P(O)(o$-$C_6H_4)PR_2$ where R$_2$ = $^iPr_2$, Cy$_2$, Et$_2$ are described. Reaction of **2aO** with MCl$_2$(cod) (M = Pd, Pt; cod = cyclooctadiene) gives products of the form [MCl(κ^1-*P*-**2aO**)(κ^2-*P,O*-**2aO**)]$^+$ Cl$^-$ and MCl$_2$(κ^2-*P,O*-**2aO**); the former exhibits fluxional behaviour which has been analysed by ^{195}Pt NMR and ^{31}P variable-temperature NMR spectroscopy. The bidentate complex is not fluxional for either the Pd or the Pt example; the Pt complex PtCl$_2$(κ^2-*P,O*-**2aO**) has been characterised by X-ray crystallography. By comparison of the product distribution seen by ^{31}P NMR spectroscopy and ESI-MS it was established that the different coordination modes of **2aO** result in quite different behaviour of the complexes when studied by ESI-MS; when the O is formally coordinated to the metal its ionisation efficiency is very low. Synthesis of Fe(CO)$_4$(**2aO**) confirmed the ability of the **2aO** ligand to render a neutral complex with no alternative pathways for ionisation to be readily detected by ESI-MS.

© 2009 Elsevier Ltd. All rights reserved.

1. Introduction

Bisphosphine monoxides (BPMOs) are an important class of hemilabile ligands [1]. The presence of both soft (P) and hard (O) Lewis base centres in one molecule allows the ligand, when complexed to a metal, to generate reactive, coordinatively unsaturated species. Dissociation of the more weakly binding donor atom provides paths to transformations at the metal centre (e.g. oxidative addition). BPMOs are capable of stabilising a wide range of transition metals, in both high and low oxidation states. The various modes of coordination of a BPMO to a metal centre are shown in Fig. 1 (along with some representative backbones), and vary depending on the nature of the metal [2].

Numerous applications exist for complexes of BPMOs [3], such as polymerisation [4], hydroformylation [5,6], hydrogenation [7], olefin hydration [8], and sulfoxidation reactions [9]. Inclusion of phosphine oxide functional groups often increases the water solubility of ligands [10] making them ideal for recovery through aqueous extraction or for catalytic transformations in water. BPMOs with non-carbon backbones have also received attention, particularly those of the form R$_2$P–N(H)–P(O)R$_2$ [11].

The bisphosphine monoxide ligand (o-C_6H_4){P(O)Ph$_2$}PPh$_2$ (dppbzO, **2aO**) has been synthesised adventitiously in small quan-

tity by hydrolysis of 1-Ph$_2$=N(SiMe$_3$)-2-(Ph$_2$P)C$_6$H$_4$ [12] and in good yield through the biphasic catalytic oxidation of dppbz [3]. The ligand has found use in Ni-catalysed ethylene oligomerisation [4,13]; the rigidity of the *o*-phenylene backbone of the phosphine ligand pre-organises the ligand for chelation and contributes to a high activation energy for β-elimination of the growing oligomer from the metal centre – proceeding through a *penta*-coordinated species – and hence to a high oligomerisation number.

There are two established synthetic routes to BPMOs [3]: combination of a phosphine and a phosphine oxide fragment, or selective oxidation of a bisphosphine. Coordination of a bisphosphine to a metal is commonly employed in selective oxidation methods [14] and although phosphines of the type R$_2$P(CH$_2$)$_n$PR$_2$ (R = alkyl) may be selectively mono-oxidised by a "protonation followed by oxidation" approach [15], aryl phosphines are less basic and require alternative synthetic routes. Applications of BPMOs with aromatic backbones are not well-developed, perhaps due to the difficulties of preparing this type of ligand. Selective catalytic mono-oxidation of dppm, dppe, dppp, dppb, dppbz, dppfc and BINAP has been demonstrated, albeit by a method which requires prior synthesis of the corresponding bisphosphine [16]. A recent and promising report of *mono*reduction of a variety of bisphosphine dioxides may provide improved access to BPMOs with aromatic backbones [17], however, it is not possible to synthesise mixed BPMOs in which the *less reactive* phosphine is oxidised (e.g. R = Ar *c.f.* R = Et) by either of these routes.

* Corresponding author. Fax: +1 250 721 7147.
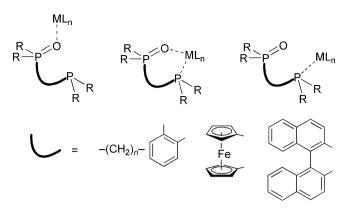*E-mail address:* mcindoe@uvic.ca (J.S. McIndoe).

Fig. 1. Modes of coordination of bisphosphine monoxide ligands. Typical R groups include Me, Ph, *p*-tolyl.

Our interest in BPMOs is due to their potential for providing high ionisation efficiencies in ESI-MS whilst coordinated to metal complexes through the phosphine fragment. Phosphine oxides ionise readily in an ESI source, typically through coordination of ions such as H^+ or Na^+ at the oxygen lone pair [18]. This "electrospray handle" would allow the complex to be readily detected in the mass spectrum and provide a facile method for characterisation [19]. We were also interested in preparing BPMOs on a reasonable scale using cheap starting materials.

Consequently we investigated *ortho*metallation of triphenylphosphine oxide (OPPh$_3$, **1O**) and subsequent reaction with an electrophile to provide *ortho*substituted products [20]; with phosphine chlorides (PR$_2$Cl) as electrophiles. Through subsequent reduction this also provides a route to bisphosphines, a class of compounds which find application in (enantioselective) [21] organometallic catalysis [22–25] and non-linear optics [26]. This paper describes the results of these experiments, the detection of byproducts, and the synthesis and characterisation of some new metal–BPMO complexes and their behaviour under ESI-MS conditions.

2. Results and discussion

2.1. Ligand syntheses

Aryl phosphine oxides react with organolithium [27] and organomagnesium [29] reagents on the aryl ring (typically *ortho* to the phosphine oxide due to intramolecular Li···O interactions) and also at the phosphorus atom. Suitable reaction conditions (reagent, temperature, solvent) depend on the acidity of proton to be abstracted, the presence of additional directing groups on the aryl ring of the phosphine oxide and possible side-reactions due to reaction at the phosphorus centre [28].
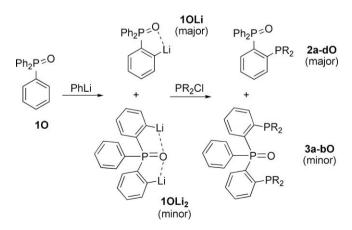
The sandwich compound Fe{η^5-C$_5$H$_4$P(O)Ph$_2$}Cp can be *ortho*metallated [29] with MgBr·N(*i*Pr)$_2$·2THF [30,31]. We found that this reaction fails for OPPh$_3$, (**1O**). Lithium diisopropylamide (LDA) [32,33], was also investigated without success. **1O** does, however, react with other alkyllithium and Grignard reagents [34,35]; and were able to successfully *ortho*lithiate **1O** with PhLi by a published method though careful adherence to experimental detail [36]. The sparing solubility of **1O** in cold diethyl ether made *stirring* essential for the 72 h reaction, and maintenance of the temperature in the range $-25\ °C \geqslant T \geqslant -35\ °C$ was also important since at temperatures much below this the titre of the PhLi solution dropped. It was necessary to use a lithium reagent bearing the same aryl group (in this case Ph) as the phosphine oxide since "scrambling" of aryl groups may occur due to the competing side-reaction of nucleophilic attack by the PhLi at the phosphorus

centre [37]. The regiochemistry of lithiation was confirmed through NMR spectroscopy studies of the product mixture following reaction with either MeI, Me$_3$SiCl or D$_2$O. Significantly, in addition to the *mono*-lithiated product, NMR spectroscopy and ESI-MS both detected evidence for *bis*-lithiated products, albeit in relatively low yield. Reaction of the lithiated **1O**, **1OLi**, with phosphine chlorides (PR$_2$Cl) proved straightforward and the steric restrictions of the synthesis were tested through use of several different phosphine chlorides (Scheme 1).

BPMO products (**2O**) were obtained in the reactions with PPh$_2$Cl (70% conversion, based on phosphine oxide, by ^{31}P NMR spectroscopy, **2aO**), PEt$_2$Cl (62%, **2bO**), PCy$_2$Cl (18%, **2cO**) and P^{i}Pr$_2$Cl (3%, **2dO**) and purified in the case of **2aO** and **2bO**. Conversion reduced as the alkyl groups on the phosphine became larger; with no detectable product following reaction with P^{t}Bu$_2$Cl. In general, ^{31}P NMR spectroscopy of **2O** products revealed doublets $\sim$30 ppm (O*P*Ph$_2$) and between -5 and -20 ppm (*P*R$_2$) with a typical $^3J_{POP} \approx 15$ Hz (see Fig. S1).

Small amounts of tris(phosphine) monoxides (TMPOs, **3aO**, **3bO**) were also obtained on reaction with PPh$_2$Cl and PEt$_2$Cl. These gave ^{31}P NMR spectroscopic signals as a triplet at low field (O*P*Ph$_2$) and a doublet at high field (2×*P*R$_2$). In the formation of these *bis*substituted products the second lithiation is suggested to have occurred on a different phenyl ring to the first, since lithiation is anticipated to deactivate the first ring towards further substitution. Double substitution provides a tantalising potential synthetic route to novel ligands containing three phosphorus centres, however, variation of the stoichiometry of the reaction between **1O** and PhLi did not significantly increase the yield of these products. Purification of the BPMOs from unreacted **1O**, PPh$_3$ (presumably arising by reaction between unreacted PhLi and PPh$_2$Cl) was performed for R = Ph and Et. The Et derivative was substantially more sensitive to aerial oxidation than the Ph, and had to be handled with corresponding care.

For R = Ph, a sample of **2aO** and **3aO** (0.4:1 ratio) containing no dioxide products by ^{31}P NMR spectroscopy showed dioxide products fairly prominently when analysed by ESI-MS (at +16 *m/z* above the original, see Fig. 2). The fully oxidised dioxides **2aO$_2$** and **3aO$_2$** therefore demonstrate a significantly higher ionisation efficiency in ESI-MS than the corresponding monoxides **2aO** and **3aO**, presumably since cation coordination is greatly enhanced by the chelate effect. Both **2aO** and **3aO** ionise by forming [M+Na]$^+$ ions in preference to [M+Li]$^+$ and by comparison to the ratio observed by NMR, **2aO** and **3aO** demonstrate a reasonably similar ionisation efficiency.

Scheme 1. General synthetic method for preparation of *ortho*-phenylene based *bis*- and *tris*(phosphine)monoxides where R = Ph (2/3aO); Et (2/3bO); Cy (2cO); ^{i}Pr (2dO). The reaction was successful for all phosphine chlorides explored except P^{t}Bu$_2$Cl. Small amounts of TPMOs were observed for PPh$_2$Cl (3aO) and PEt$_2$Cl (3bO).
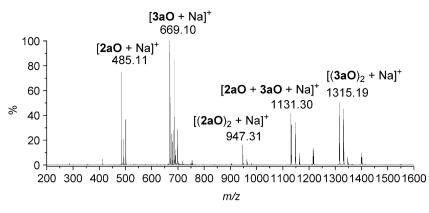
Fig. 2. ESI-MS (CH$_2$Cl$_2$/MeOH) of a 0.4:1 mixture of **2aO/3aO** showing the nature of aggregation under soft ionisation conditions and the enhanced detection of dioxide products (not seen by NMR) at 16 *m/z* units above the monoxide peak.

This synthetic method opens a route to relatively expensive bisphosphines such as **2a** (dppbz); mono or bisphosphine oxides may be reduced by methods typically employing hydrides such as diisobutylaluminium hydride (DIBAL-H) [38] or LiAlH$_4$ [39,40] and silanes such as phenylsilane [41] and trichlorosilane [42–45]. **2aO** is readily reduced to **2a** with HSiCl$_3$/P(OEt)$_3$, as expected (Fig. S2).

2.2. Metal complexes

Catalysts employing phosphine ligands are commonly synthesised *in situ*, from a catalyst precursor and the free ligand. We investigated the product distribution formed by reaction of **2aO** with both Pt^{II} and Pd^{II} species (Scheme 2) by NMR spectroscopy and compared this with the product distribution detected by ESI-MS.
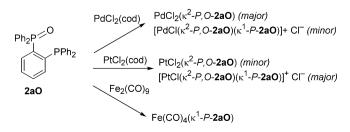
2.3. Reaction with PtCl$_2$(cod)

The ^{31}P NMR spectrum at 294 K of the mixture formed by reaction of PtCl$_2$(cod) with **2aO** revealed two main products (plus a small amount of free ligand); [PtCl(κ^1-*P*-**2aO**)(κ^2-*P,O*-**2aO**)]$^+$ Cl$^-$ and PtCl$_2$(κ^2-*P,O*-**2aO**) in approximately a 4:1 ratio, with the former exhibiting fluxional behaviour. The reactivity seen for **2aO** shows similarities to the chelating "PAN" ligand 1-(dimethylamino)-8-(diphenylphosphino)naphthalene, which reacts with both Pt^{II} and Pd^{II} to form bidentate and monodentate complexes [46], and BINAP(O) which has been shown to coordinate in both κ^1 and κ^2 denticities to Pd [47].

2.4. [PtCl(κ^1-P-2aO)(κ^2-P,O-2aO)]$^+$ Cl$^-$

2.4.1. ^{31}P NMR spectroscopy

At ambient temperature the coordinated phosphine groups are equivalent, with a single resonance at 7.9 ppm with ^{195}Pt satellites and $^1J_{PtP}$ of 4152 Hz. The two phosphine oxide groups (P$_B$) exchanged rapidly, corresponding to a broad resonance at 35.4–

45.4 ppm. On cooling the signal at 7.9 ppm split into two separate resonances; at 198 K these were seen at 9.9 ppm (P$_C$, $^1J_{PtP}$ 4524 Hz) and 7.8 ppm (P$_E$, $^1J_{PtP}$ 3736 Hz). The fluxionality is thought to be due to the lability of the phosphine oxide groups, the symmetry of the complex being broken when one phosphine oxide is metal-bound and one is dissociated (Fig. 3; only the *T* range 240–300 K is shown). NOESY and COSY experiments at 190 K confirmed that P$_E$ and P$_F$ are within the same ligand, likewise with P$_C$ and P$_D$. The resonance corresponding to P$_D$ is seen at 32.8 ppm, similar to the PO group of uncomplexed **2aO** (29–32 ppm depending on solvent) indicating that the interaction of this phosphine oxide group with the metal centre is reduced at low temperature. At low temperature small ($^2J_{POP}$ 16 Hz, P$_E$ to P$_C$; $^3J_{PP}$ 8 Hz, P$_E$ to P$_F$) couplings were seen for the κ^2-bound ligand (P$_E$, P$_F$); for the κ^1-bound ligand (P$_C$, P$_D$) the corresponding coupling ($^2J_{POP}$ 16 Hz, P$_C$ to P$_E$) was seen, this modest value is consistent with a *cis* rather than *trans* arrangement of phosphine ligands [48]. For complexes of **2aO** we generally observed that the $^3J_{PP}$ coupling of **2aO** is lost if the phosphine oxide group is not coordinated to the metal centre, presumably because twisting of the ligand affects the through-bond coupling; a lack of detectable $^3J_{PP}$ coupling between P$_C$ and P$_D$ at low temperature was consistent with this. Essentially, cooling of the sample leads to the hemilability of the ligand being frozen out. The mechanism by which the exchange occurs is not known; the intermediate may involve a three-coordinate [PtP$_2$Cl]$^+$ species, or a four-coordinate [PtP$_2$O$_2$]$^{2+}$ species.

2.4.2. ^{195}Pt NMR spectroscopy

At 294 K a pseudo-triplet (doublet of doublets) was seen at −3971 ppm corresponding to [PtCl(κ^1-*P*-**2aO**)(κ^2-*P,O*-**2aO**)]$^+$ Cl$^-$ (see Fig. S2), consistent with reports of similar compounds [49]. This relates to a Pt species bonded to two nearly equivalent phosphine ligands at room temperature; the $^1J_{PtP}$ of 4159 Hz correlating well with the corresponding P$_A$ $^1J_{PPt}$ coupling of 4152 Hz in the ^{31}P NMR spectrum. These values are larger than the typical range for $^1J_{Pt-P}$ couplings in *trans* complexes (2400–3000 Hz) [50] reflecting the increased bond strength of the Pt–P bonds in the *cis* complex [51,52].

2.4.3. PtCl$_2$(κ^2-P,O-2aO)

PtCl$_2$(κ^2-*P,O*-**2aO**) was not fluxional over the temperature range studied (190–300 K). Two doublets (P$_X$, P$_Y$) were seen in the ^{31}P NMR spectrum, the coordinated phosphine P$_X$ showing ^{195}Pt satellites ($^1J_{PPt}$ 3770 Hz). The ^{195}Pt NMR spectrum showed a corresponding doublet at −3085 ppm ($^1J_{PtP}$ = 3771 Hz) (Fig. S3) indicating that only one BPMO ligand was attached to the metal centre.
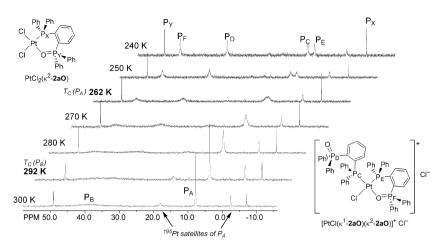
Scheme 2. Routes to metal complexes of the bisphosphine monoxide ligand **2aO**.

Fig. 3. Variable temperature ^{31}P NMR (202 MHz) spectra of PtCl$_2$(κ^2-**2aO**) and [PtCl$_2$(κ^1-P-**2aO**)(κ^2-**2aO**)]$^+$ Cl$^-$. P$_C$ and P$_E$ coalesce into P$_A$ at 262 K, and P$_D$ and P$_F$ coalesce into P$_B$ at 292 K.
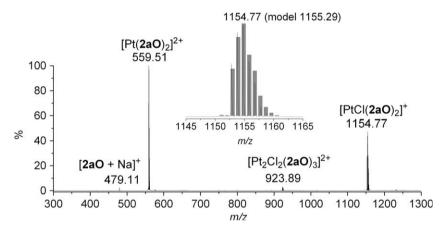

Fig. 4. ESI-MS (CH$_2$Cl$_2$/MeCN) of reaction between PtCl$_2$(cod) and **2aO**. The inset spectrum shows the overlaid experimental and calculated isotope patterns for [PtCl(**2aO**)$_2$]$^+$.

2.5. Mass spectrometric analysis of Pt complexes

A primary motivation for this work was to establish the performance of BPMOs in improving ESI-MS analysis of metal complexes. We investigated the ability of the phosphine oxide to associate with charged species when the PO is pendant (κ^1) or coordinated to a metal centre (κ^2) and also the competition between ionisation through cation coordination and alternative ionisation pathways. ESI-MS analysis of the mixture of [PtCl(κ^1-P-**2aO**)(κ^2-P,O-**2aO**)]$^+$ Cl$^-$ and PtCl$_2$(κ^2-P,O-**2aO**) showed derivatives of the former only (Fig. 4), as the complex is ionised in solution. The cation [PtCl(**2aO**)$_2$]$^+$ (MS gives no information on the mode of bonding of the ligand) is observed, as is the dication [Pt(**2aO**)$_2$]$^{2+}$ – presumably generated through chloride loss from the monocation during the electrospray ionisation process. Halide loss to form [M−X]$^+$ or [M−2X]$^{2+}$ ions is a well-documented ionisation pathway for metal halide complexes [53,54]. In this case we suggest that the additional pendant phosphine oxide group is responsible for facilitating chloride loss through intramolecular stabilization of this coordinatively unsaturated species. In comparison, the neutral PtCl$_2$(κ^2-P,O-**2aO**) is only barely detected (0.2% intensity) as an [M+Na]$^+$ ion at 751.00 m/z; no [M−Cl]$^+$ ion was observed for this compound. The only other sodiated ion present was the free ligand, [2aO+Na]$^+$, whose appearance is consistent with the ^{31}P NMR spectroscopic results. The dicationic peak at 923.89 m/z is assignable to [Pt$_2$Cl$_2$(**2aO**)$_3$]$^{2+}$ (confirmed by MS/MS), a species that is probably

present at low concentration and hence not detected by NMR spectroscopy, or which may form under the conditions of electrospray ionisation. A reasonable dimeric structure can be envisaged for [Pt$_2$Cl$_2$(**2aO**)$_3$]$^{2+}$, in which the chloride ligands bridge between the two Pt centres.

2.6. Fragmentation studies

MS/MS fragmentation pathways were studied using EDESI-MS/MS. This involves collecting spectra over a wide range of collision energies and combining all the results into a single map in which ion intensity is contoured (see Fig. S5 for example) [55]. Such maps make interpretation of complex fragmentation pathways considerably easier [56]. Product ions formed by fragmentation of the most abundant ions, [Pt$_2$Cl$_2$(**2aO**)$_3$]$^{2+}$, [Pt(**2aO**)$_2$]$^{2+}$ and [PtCl(**2aO**)$_2$]$^+$, are shown in Fig. 5.

2.7. Fragmentation of [PtCl(2aO)$_2$]$^+$

Fragmentation of [PtCl(**2aO**)$_2$]$^+$ involves decomposition by three different pathways (Fig. 5a). Transfer of Ph$^-$ from the phosphine ligand to the platinum complex generates the charged product ion [**2aO**− Ph]$^+$ at 385.1 m/z in the lowest energy fragmentation pathway. Alternatively, loss of HCl from the precursor complex gives [Pt(**2aO**)$_2$−H]$^+$ at 1119.0 m/z. The highest energy fragmentation of [PtCl(**2aO**)$_2$]$^+$ involves loss of an uncharged **2aO** ligand to give
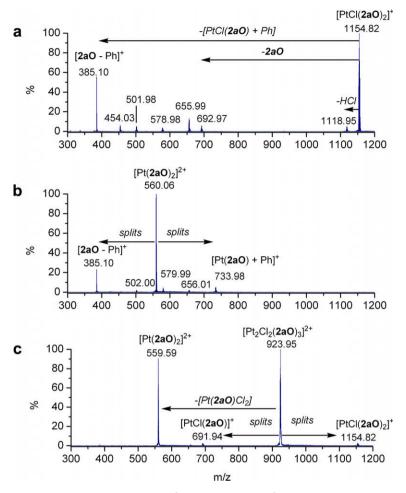
Fig. 5. MS/MS of (a) [PtCl(**2aO**)$_2$]$^+$, (b) [Pt(**2aO**)$_2$]$^{2+}$ and (c) [Pt$_2$Cl$_2$(**2aO**)$_3$]$^{2+}$ species seen in the ESI-MS spectrum.

[PtCl(**2aO**)]$^+$ at 693.0 *m/z*, rapidly followed by loss of HCl to give [Pt(**2aO**)−H]$^+$ at 656.0 *m/z*. This latter species fragments further at a higher collision energy through sequential loss of two Ph$^•$ groups and PO$^•$ to give the last detectable fragment [Pt(**2aO**)−POPh$_2$H]$^+$ at 454.0 *m/z*. As cations do not commonly fragment through anion loss to form dications, it is unsurprising that fragmentation of [PtCl(**2aO**)$_2$]$^+$ does not produce [Pt(**2aO**)$_2$]$^{2+}$.

2.8. Fragmentation of [Pt(2aO)$_2$]$^{2+}$

The dication [Pt(**2aO**)$_2$]$^{2+}$ detected under MS/MS conditions at 560.1 *m/z* fragments to produce two singly charged product ions by transfer of a phenyl group from one ligand to Pt to form [Pt(**2aO**)+Ph]$^+$ at 734.0 *m/z* and elimination of the phosphonium ion [**2aO**− Ph]$^+$, seen at 385.1 *m/z* (Fig. 5b). This fragmentation pathway is outlined pictorially in Fig. 6.

At higher collision energies minor fragments are seen which correspond to the loss of a neutral ligand plus smaller fragments; these species are seen: [Pt(**2aO**− 2Ph)]$^+$, 502.0 *m/z*; [Pt(**2aO**)−Ph]$^+$, 580.0 *m/z*; and [Pt(**2aO**)−H]$^+$, 656.0 *m/z*. The absence in the MS/MS spectrum of species such as [**2aO**+H]$^+$ and [**2aO**+Ph]$^+$ indicate that the neutral ligand and the smaller fragments (H$^+$, Ph$^+$) are lost separately.

2.9. Fragmentation of [Pt$_2$Cl$_2$(2aO)$_3$]$^{2+}$

MS/MS of [Pt$_2$Cl$_2$(**2aO**)$_3$]$^{2+}$ reveals two fragmentation pathways (Fig. 5c). The major route (pathway **A**) involves loss of neutral PtCl$_2$(**2aO**) to form [Pt(**2aO**)$_2$]$^{2+}$, and in the other (**B**), the dication
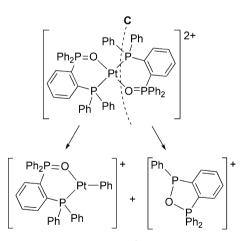

Fig. 6. Putative structure of the [Pt(**2aO**)$_2$]$^{2+}$ species (the *cis* version is equally likely) and its primary fragmentation pathway.

divides into two monocations, [PtCl(**2aO**)$_2$]$^+$ and [PtCl(**2aO**)]$^+$ each retaining one chloride ligand. Both pathways are consistent with the dimeric structure postulated for [Pt$_2$Cl$_2$(**2aO**)$_3$]$^{2+}$ which is shown in Fig. 7.

2.10. X-ray crystallography

Yellow crystals grown by vapour diffusion (pentane/CH$_2$Cl$_2$) were characterised by single-crystal X-ray diffraction and were
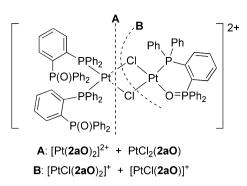
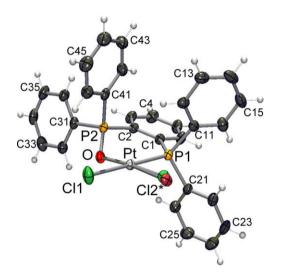**Fig. 7.** Putative structure of the $[Pt_2Cl_2(\mathbf{2aO})_3]^{2+}$ species and its fragmentation pathways.

Fig. 8. ORTEP plot of $PtClX(\kappa^2\text{-}P,O\text{-}\mathbf{2aO})\cdot CH_2Cl_2$ (X = Cl, 70%; Br, 30%). CH_2Cl_2 of crystallisation not shown, non-hydrogen atoms are represented by Gaussian ellipsoids at the 50% probability level. Hydrogen atoms are shown with arbitrarily small thermal parameters. Selected bond lengths (Å): Pt–Cl(1) 2.3567(8); Pt–Cl(2) 2.269(10); Pt–P(1) 2.2147(7); Pt–O 2.060(2); P(1)–C(1) 1.839(3); P(2)–O 1.521(2); P(2)–C(2) 1.801(3); C(1)–C(2) 1.402(4). Selected bond angles (°): Cl(1)–Pt–Cl(2) 91.44(4); Cl(1)–Pt–O 85.74(6); Cl(2)–Pt–P(1) 87.1(4); Cl(2)–Pt–O 176.2(4); P(1)–Pt–O 95.74(6); Pt–P(1)–C(1) 116.05(10); O–P(2)–C(2) 111.95(13); Pt–O–P(2) 116.15(11); P(1)–C(1)–C(2) 124.4(2); P(2)–C(2)–C(1) 122.5(2).

shown to consist of the *mono*substituted product $PtCl_2(\kappa^2\text{-}P,O\text{-}\mathbf{2aO})$ co-crystallised 1:1 with CH_2Cl_2 solvent (CCDC 699942). X-ray crystallographic parameters for $PtCl_2(\kappa^2\text{-}P,O\text{-}\mathbf{2aO})$ are given in Table S1. The molecular structure of $[PtCl_2(\kappa^2\text{-}P,O\text{-}\mathbf{2aO})]$ is given in Fig. 8 along with key bond lengths and angles. The Pt site *trans* to oxygen contained a mixture of Cl and Br (70% and 30%, respectively; the Br is presumed to originate from the PhLi/LiBr solution used in the ligand synthesis). Coordination of $\mathbf{2aO}$ to Pt in a bidentate fashion does not impose a great deal of strain on the $\mathbf{2aO}$ ligand, the torsion angle of $-0.83°$ P(2)–C(2)–C(1)–P(1) indicating that the central benzene ring is essentially undistorted and the bite angle at Pt is $\sim96°$. Pt–P (2.2147 Å) and Pt–O (2.060 Å) bond distances are consistent with similar structures [57].

2.11. Reaction with $PdCl_2(cod)$

The reaction between $\mathbf{2aO}$ and $PdCl_2(cod)$ gave both κ^1- and κ^2-products, although in contrast to the Pt derivatives, $PdCl_2(\kappa^2\text{-}P,O\text{-}\mathbf{2aO})$ was the major product (2:1 ratio) compared to the *bis*substituted fluxional complex $[PdCl(\kappa^1\text{-}P\text{-}\mathbf{2aO})(\kappa^2\text{-}P,O\text{-}\mathbf{2aO})]^+$ Cl^-. This product selection may be due to the slightly harder Pd

coordinating the oxygen more strongly, favouring the formally bound $PdCl_2(\kappa^2\text{-}P,O\text{-}\mathbf{2aO})$ complex, whereas the softer Pt favours coordination of the two P groups in $PtCl_2(\kappa^1\text{-}P\text{-}\mathbf{2aO})_2$. The regiochemistry of $[PdCl(\kappa^1\text{-}P\text{-}\mathbf{2aO})(\kappa^2\text{-}P,O\text{-}\mathbf{2aO})]^+$ Cl^- was assigned as the P donors coordinating *cis* rather than *trans* based on the modest $^2J_{PP}$ coupling of 23 Hz at low temperature. A comprehensive review of the literature places $^2J_{PP}$ *cis* couplings for Pd^{II} *bis*phosphine complexes in the range -25 to $+80$ Hz [58], and *trans* couplings in the range $+441$ to $+1269$ Hz [59]. Since the behaviour for Pd is reasonably similar to that observed for Pt, representative VT ^{31}P NMR spectral and ESI-MS data for the Pd derivatives are shown in the supporting information.

Despite the differences in speciation seen by ^{31}P NMR spectroscopy for Pd *vs* Pt on complexation of $\mathbf{2aO}$, the ESI-MS speciation appeared largely the same (Fig. S4). The $PdCl_2(\kappa^2\text{-}P,O\text{-}\mathbf{2aO})$ species was – as in the Pt case – only weakly represented in the ESI-MS (as the $[M+Na]^+$ adduct) despite being shown by ^{31}P NMR spectroscopy to be the major product formed.

2.12. $Fe(CO)_4(\kappa^1\text{-}P\text{-}2aO)$

$Fe(CO)_4(\kappa^1\text{-}P\text{-}\mathbf{2aO})$, which has no overall charge and which does not possess an ionisation pathway (such as loss of Cl^- which was possible for the Pt and Pd species) except for coordination of a positive ion (e.g. Li^+, Na^+, H^+) through the phosphine oxide, was prepared from $\mathbf{2aO}$ and $Fe_2(CO)_9$. ^{31}P NMR spectroscopy showed that the complex was not fluxional, and furthermore, the chemical shift of the phosphine oxide group (δ_P: 29.9 ppm) is similar to that of the free ligand suggesting that it is completely uninvolved with the metal centre. By ESI-MS, $Fe(CO)_4(\kappa^1\text{-}P\text{-}\mathbf{2aO})$ was seen exclusively as $[M+M']^+$ where $M' = Na^+$ or H^+; Li^+ and NH_4^+ adducts were not detected. MS/MS analysis showed the sequential loss of CO ligands with a competing fragmentation pathway involving loss of $Fe(CO)_4$ to leave just the charged ligand $[\mathbf{2aO}+Na]^+$ at 485 m/z (Fig. S6). The ESI-MS also shows evidence for higher aggregates such as $Fe_2(CO)_4(\mathbf{2aO})_2$ that are not observed in the ^{31}P NMR spectra; possibly they are only present in trace amounts.

3. Experimental

3.1. General

Dry, reagent grade solvents were obtained by distillation or from a solvent purification system. Reagents were purchased from Strem and Aldrich and used without further purification. Reactions were performed under nitrogen using standard Schlenk techniques. Silica columns were loaded and run under nitrogen. Electrospray ionisation mass spectra were collected using a Micromass QTof *micro* instrument (cone voltage 15 V, nebuliser tip 3100 V, nitrogen desolvation gas 80 °C). Data collection was carried out in MCA mode for MS spectra and continuum mode for MS/MS and EDESI spectra. NMR spectra were recorded on the following Bruker spectrometers: AV-500, AC-300 or AMX-360. Chemical shifts are quoted in δ (ppm) referenced to residual solvent resonances (^1H, ^{13}C) or external references of 85% aqueous H_3PO_4 (^{31}P). Heteronuclear NMR spectra were run with non-deuterated solvents and an internal sealed glass capillary (a lock stick) containing D_2O allowing samples to be easily made up in a glovebox. Assignments were assisted by $^1H\{^{31}P\}$, ^{31}P and ^1H NOESY and COSY experiments, ^{13}C-DEPT, ^1H–^{13}C-HSQC and ^1H–^{13}C-HMBC NMR experiments. ^{13}C NMR assignments were consolidated by running experiments on AV-500 and AC-300 instruments and comparing ^{31}P–^{13}C coupling. Full assignment of ^{13}C spectra was not possible in all cases due to the complexity of the ^{31}P–^{13}C coupling. A 5 s delay was used on ^{31}P NMR spectra, despite this it was

observed that there was a small consistent and reproducible integration error, with PR$_3$ groups being slightly underrepresented compared to P(O)R$_3$. Melting points were recorded on a Gallenkamp MPA and are uncorrected. IR spectra were recorded using a solution cell on a Perkin–Elmer 1000 FTIR spectrometer. X-ray crystallography data for PtClX(κ^2-P,O-**2aO**)·CH$_2$Cl$_2$ was collected in the X-ray Laboratory of the University of Alberta Chemistry Department. Measurements were made at −80 °C on a Bruker PLATFORM/SMART 1000 CCD diffractometer with Mo Kα radiation (λ = 0.71073 Å). The structure was solved by direct methods and unit cell parameters were obtained from full-matrix least-squares refinement on F^2. All fully oxidised phosphines (including **1O**) were obtained through oxidation with H$_2$O$_2$ [60].

3.1.1. Lithiation of triphenylphosphine oxide (**1O**)

An ethereal phenyllithium solution [61,62] (0.6–0.9 M) was cooled to −25 °C using an acetone/CO$_2$ bath. To this solution **1O** (1eq.) was added using a solid-addition device. The brown suspension was stirred in a freezer (−25 °C) for 72 h to give an opaque orange solution of **1OLi**.

3.1.2. Reaction of **1OLi** with PPh$_2$Cl; isolation of **2aO** and **3aO**; oxidation of **2aO** to **2aO$_2$**

PPh$_2$Cl (2.9 ml, 15.7 mmol) was added to a stirred solution of **1OLi** (23.5 ml, 0.65 M, 15.3 mmol) at −25 °C and the solution allowed to warm to 23 °C overnight with stirring. The resulting yellow solution/cream precipitate consisted of a mixture of **2aO** and **3aO**. THF (10 ml) and 1,2-dichloroethane (30 ml) were added to dissolve the product. The solution was washed (H$_2$O, 2 × 20 ml), NaCl$_{(aq)}$ (2 × 20 ml) and the solvent removed before redissolving the residue in minimal CH$_2$Cl$_2$ and purifying by silica column chromatography (2:1 CH$_2$Cl$_2$/AcOEt). **2aO** was isolated as white foamy solid R_f 0.48 (yield 3.03 g, 6.5 mmol, 47%), and **3aO** as a white solid; R_f 0.68 (yield 0.30 g, 0.46 mmol, 3%). **2aO** was oxidised with H$_2$O$_2$ to give **2aO$_2$** which was isolated by precipitation from CH$_2$Cl$_2$/pentane. See supporting information for assignment of structures **2aO** and **3aO** and spectroscopic details.

3.1.3. Reduction of **2aO** to **2a**

A pressure tube containing **2aO** (0.092 g, 0.2 mmol) was evacuated and placed under N$_2$ (conducted behind a blast shield). THF (3 ml) and toluene (3 ml) were added and the solid stirred to dissolution. The solution was freeze-pump-thaw degassed (6 cycles). Triethylphosphite (0.33 ml, 2.0 mmol) and HSiCl$_3$ (0.8 ml, 8 mmol) were added with stirring. The solution was frozen, the headspace evacuated and the tube sealed. The solution heated to 100 °C and stirred (88 h). Ether (10 ml) was added and an aliquot of the solution was filtered and analysed by ^{31}P NMR. The solvent was removed and replaced with CDCl$_3$ for further analysis.

3.1.4. Reaction of **1OLi** with PR$_2$Cl; oxidation of **2bO** to **2bO$_2$**

PEt$_2$Cl (0.3 ml, 0.31 g, 2.5 mmol) was measured into a flask in the glovebox, stoppered and removed. Dry ether (10 ml) was added and the temperature reduced to −78 °C. The solution was stirred and an ethereal solution of **1OLi** was added (2.5 ml, 2.3 mmol). The solution was allowed to warm to room temperature overnight with stirring (^{31}P NMR yield, **2bO**: 62%, **3bO**: 6%). The solvent was removed under vacuum and the residue extracted with fluorobenzene (3 × 5 ml). The solvent was removed and the residue washed with hexane (1 × 5 ml) and then extracted with toluene (4 × 5 ml). The highly air-sensitive product **2bO** crystallised as a white solid (0.25 g, 0.68 mmol, 30%). **2bO** and **3bO** were oxidised with H$_2$O$_2$ to **2bO$_2$** and **3bO$_3$**, respectively. **2cO** and **2dO** were prepared in analogous fashion in yields of 18% and 3%, respectively.

3.1.5. [PtCl(κ^1-P-2aO)(κ^2-P,O-2aO)]$^+$ Cl$^-$ and PtCl$_2$(κ^2-P,O-2aO)

PtCl$_2$(cod) (0.0106 g, 0.028 mmol) [63] and **2aO** (0.026 g, 0.06 mmol, 2 eq.) were stirred in CH$_2$Cl$_2$ (3 ml) for 2 h. Pentane was added and the solution was left overnight at 5 °C, forming a microcrystalline yellow precipitate. The product distribution in the reaction solution consisted of [PtCl(κ^1-P-**2aO**)(κ^2-P,O-**2aO**)]$^+$ Cl$^-$ and PtCl$_2$(κ^2-P,O-**2aO**) in a 4:1 ratio (as determined by ^{31}P NMR).

3.1.6. [PdCl(κ^1-P-2aO)(κ^2-P,O-2aO)]$^+$ Cl$^-$ and PdCl$_2$(κ^2-P,O-2aO)

A CH$_2$Cl$_2$ (3 ml) solution of PdCl$_2$(cod) (0.035 g, 0.04 mmol) and **2aO** (0.034 g, 0.074 mmol) was stirred at 23 °C for 2 h. For ^{31}P VT NMR samples an aliquot of the reaction mixture was taken after 2 h and CD$_2$Cl$_2$ added as lock. If the original solution was left to sit overnight an orange/yellow precipitate formed which was isolated by suction filtration (0.038 g), washed with acetone and recrystallised from CH$_2$Cl$_2$/pentane by vapour diffusion. Yellow prisms formed, but were of insufficient quality for X-ray diffraction studies. The products formed in the ratio 1:0.54 for [PdCl(κ^1-P-**2aO**)(κ^2-P,O-**2aO**)]$^+$ Cl$^-$:PdCl$_2$(κ^1-P-**2aO**)$_2$ (as determined by ^{31}P NMR).

3.1.6.1. Fe(CO)$_4$(κ^1-P-2aO).

Fe$_2$(CO)$_9$ (0.03 g, 0.08 mmol) was measured into a 2-neck flask (glovebox), stoppered and removed. Dry THF was added (1.5 ml) followed by **2aO** (0.037 g, 0.08 mmol) in dry THF (0.5 ml). The resulting solution was heated at 60 °C for 2.5 h with stirring, followed by cooling and removal of the solvent to give a red residue. Under inert atmosphere the residue was extracted with dry hexane (3 ml), which was then filtered to give a bright yellow solution of Fe(CO)$_4$(κ^1-P-**2aO**) and unreacted **2aO**.

4. Conclusions

A route to a class of known and novel BPMOs via *ortho*lithiation of triphenylphosphine oxide has been presented. Although only modest conversions have been reported, and steric factors are clearly an important limitation, the method involves cheap, readily available materials and can be carried out on an appreciable scale with sterically undemanding dialkylhalophosphines to access new and known BPMOs, including those in which the least reactive phosphine is the oxidised group. Under mass spectrometric conditions the BPMO ligand **2aO** shows high affinity for H$^+$ and Na$^+$; the particular preference of one or the other is thought to depend on cation availability in the instrument. ^{31}P NMR spectroscopy of the reaction of **2aO** with PtCl$_2$(cod) and PdCl$_2$(cod) reveals that a κ^1/κ^2 fluxional mode of coordination is favoured for Pt, whereas a κ^2 non-fluxional mode is favoured for Pd. In Fe(CO)$_4$(κ^1-P-**2aO**) the phosphine oxide appears to be uninvolved with the Fe^0 metal centre. Detection of metal-bound **2aO** species by ESI-MS depends largely on the availability of the phosphine oxide lone pair for cation coordination; when bound in a κ^2-mode e.g. MCl$_2$(κ^2-P,O-**2aO**) (M = Pd, Pt) the complexes are only faintly detected by ESI-MS (even when, in the case of Pd, the complex is the major product of the reaction) suggesting that the lone pairs of the phosphine oxide are significantly involved in bonding to the metal centre. Analysis of the X-ray crystallographic data of PtCl$_2$(κ^2-P,O-**2aO**) shows the Pt–O bond distance (2.060 Å) to be comparable with that of other Pt-bound phosphine oxide ligands. Promotion of Cl$^-$ loss as demonstrated by **2aO** in κ^1-bound complexes show it to be an ideal candidate for reversible stabilisation of a metal centre through the phosphine oxide group, a feature which is highly desirable for catalytic transformations. The affinity of the PO group for cations is very low when formally κ^2-bound, although it was still possible to detect these complexes at low abundance by ESI-MS.

We therefore conclude that **2aO** has shown some potential as an electrospray-active ligand to make complexes more amenable to detection by ESI-MS particularly under circumstances where no other ionisation pathways are available. However, the coordinating power of the P=O group means that the ligand has a strong propensity to act as a hemilabile ligand, with both P and O binding to the metal in chelating fashion. We note that dioxide forms such as **2aO$_2$** show disproportionately strong signals in the mass spectrum. If derivatised with a phosphine at a further position on the ring (e.g. by repeating the ortholithiation step to make species such as **3aO$_2$**) it is envisaged that such trisphosphine dioxides would also make highly effective electrospray-active ligands.

Acknowledgments

Appendix A. Supplementary data

Additional characterisation: ^{13}C NMR spectra, X-ray crystallographic parameters, ^{31}P NMR spectra, ^{195}Pt NMR spectrum, VT ^{31}P NMR spectra, ESI-MS, EDESI-MS, ESI-MS/MS. Supplementary data associated with this article can be found, in the online version, at doi:10.1016/j.poly.2009.08.013.

References

[1] V.V. Grushin, Chem. Rev. 104 (2004) 1629.
[2] I. Brassat, U. Englert, W. Keim, D.P. Keitel, S. Killat, G. Suranna, R. Wang, Inorg. Chim. Acta 280 (1998) 150.
[3] (a) V.V. Grushin, Organometallics 20 (2001) 3950;
(b) S.J. Higgins, R. Taylor, B.L. Shaw, J. Organomet. Chem. 325 (1987) 285;
(c) S.A. Al-Jibori, Z.M. Kalay, T.A.K. Al-Allaf, Trans. Met. Chem. 19 (1994) 293;
(d) S.A. Al-Jibori, O.H. Amin, T.A.K. Al-Allaf, R. Davis, Trans. Met. Chem. 16 (2001) 186;
(e) R.J. Coyle, Y.L. Slovokhotov, M.Y. Antipin, V.V. Grushin, Polyhedron 17 (1998) 3059.
[4] I. Brassat, W. Keim, S. Killat, M. Möthrath, P. Mastrorilli, C.F. Nobile, G.P. Suranna, J. Mol. Catal. A: Chem. 157 (2000) 41.
[5] (a) C. Abu-Gnim, I. Amer, J. Organomet. Chem. 516 (1996) 235;
(b) D.D. Ellis, G. Harrison, A.G. Orpen, H. Phetmung, P.G. Pringle, J.G. deVries, H. Oevering, J. Chem. Soc., Dalton Trans. 5 (2000) 671.
[6] (a) R. Weber, U. Englert, B. Ganter, W. Keim, M. Möthrath, J. Chem. Soc., Chem. Commun. 15 (2000) 1419;
(b) C. Roch-Neirey, N. Le Bris, P. Laurent, J.-C. Clément, H. des Abbayes, Tetrahedron Lett. 42 (2001) 643.
[7] P.W. Cyr, S.J. Rettig, B.O. Patrick, B.R. James, Organometallics 21 (2002) 4672.
[8] N.D. Jones, B.R. James, Can. J. Chem. 83 (2005) 546.
[9] P. Sgarbossa, E. Pizzo, A. Scarso, S.M. Sbovata, R.A. Michelin, M. Mozzon, G. Strukul, F. Benetollo, J. Organomet. Chem. 69 (2006) 3659.
[10] T.L. Schull, J.C. Fettinger, D.A. Knight, Inorg. Chem. 35 (1996) 6717.
[11] M.B. Smith, A.M.Z. Slawin, J.D. Woollins, Polyhedron 15 (1996) 1579.
[12] R.W. Reed, B. Santarsiero, R.G. Cavell, Inorg. Chem. 35 (1996) 4292.
[13] G.W. Parshall, Homogeneous Catalysis – The Applications and Chemistry of Catalysis by Soluble Transition Metal Complexes, first ed., vol. 4, Wiley, 1980, 56–61.
[14] W.-C. Yeo, L. Tang, B. Yan, S.-Y. Tee, L.L. Koh, G.-K. Tan, P.-H. Leung, Organometallics 24 (2005) 5581.
[15] P. Mäding, D. Scheller, Z. Anorg. Allg. Chem. 567 (1988) 179.
[16] V.V. Grushin, J. Am. Chem. Soc. 121 (1999) 5831.
[17] M.J. Petersson, W.A. Loughlin, I.D. Jenkins, Chem. Commun. 37 (2008) 2293.
[18] This is true to the point that the common solvent HMPA has to be excluded from the instrument due to its ability to contaminate the instrument, producing persistent [M(HMPA)$_n$]$^+$ (M = H, Na, K; n = 1–4) ions.
[19] (a) C. Decker, W. Henderson, B.K. Nicholson, J. Chem. Soc., Dalton Trans. 19 (1999) 3507;
(b) N.J. Farrer, R. McDonald, J.S. McIndoe, J. Chem. Soc., Dalton Trans. 38 (2006) 4570.
[20] (a) For reviews see J. Clayden, Chem. Organolithium Compd. 1 (2004) 495;
(b) V. Snieckus, Chem. Rev. 90 (1990) 879.
[21] N.V. Dubrovina, V.I. Tararov, A. Monsees, R. Kadyrov, C. Fischer, A. Börner, Tetraheron: Asymmetry 14 (2003) 2739.
[22] L.F. Warren, M.A. Bennett, Inorg. Chem. 15 (1976) 3126.
[23] S.C. Grocott, S.B. Wild, Inorg. Chem. 21 (1982) 3526.
[24] W. Levason, M.L. Matthews, B. Patel, G. Reid, M. Webster, J. Chem. Soc., Dalton Trans. 20 (2004) 3305.
[25] M.F. Davis, M. Clarke, W. Levason, G. Reid, M. Webster, Eur. J. Inorg. Chem. 14 (2006) 2773.
[26] A.M. McDonagh, M.P. Cifuentes, M.G. Humphrey, S. Houbrechts, J. Maes, A. Persoons, M. Samoc, B. Luther-Davies, J. Organomet. Chem. 610 (2000) 71.
[27] D. Seyferth, D.E. Welch, J.K. Heeren, J. Am. Chem. Soc. 86 (1964) 1110.
[28] J. Clayden, Tetrahedron Organic Chemistry Series Elsevier 23 (2002).
[29] U. Nettekoven, M. Widhalm, P.C.J. Kamer, P.W.N.M. van Leeuwen, K. Mereiter, M. Lutz, A.L. Spek, Organometallics 19 (2000) 2299.
[30] P.E. Eaton, C. Lee, Y. Xiong, J. Am. Chem. Soc. 111 (1989) 8016.
[31] K.W. Henderson, W.J. Kerr, Chem. Eur. J. 7 (2001) 3430.
[32] R. Schmid, J. Foricher, M. Cereghetti, P. Schönholzer, Helv. Chim. Acta 74 (1991) 370.
[33] K.J. Singh, D.B. Collum, J. Am. Chem. Soc. 128 (2006) 13753.
[34] H. Gilman, G.E. Brown, J. Am. Chem. Soc. 67 (1945) 824.
[35] O. Desponds, C. Huynh, M. Schlosser, Synthesis 7 (1998) 983.
[36] O. Desponds, M. Schlosser, J. Organomet. Chem. 507 (1996) 257.
[37] J.P. Henschke, A. Zanotti-Gerosa, P. Moran, P. Harrison, B. Mullen, G. Casy, I.C. Lennon, Tetrahedron Lett. 44 (2003) 4379.
[38] C.A. Busacca, J.C. Lorenz, N. Grinberg, N. Haddad, M. Hrapchak, B. Latli, H. Lee, P. Sabila, A. Saha, M. Savestani, S. Shen, R. Varsolona, X. Wei, C.H. Senanayake, Org. Lett. 7 (2005) 4277.
[39] R. Shintani, K. Yashio, T. Nakamura, K. Okamoto, T. Shimada, T. Hayashi, J. Am. Chem. Soc. 128 (2006) 2772.
[40] T. Imamoto, S. Kikuchi, T. Miura, Y. Wada, Org. Lett. 3 (2001) 87.
[41] T. Miura, T. Imamoto, Tetrahedron Lett. 40 (1999) 4833.
[42] (a) Literature concerning silane reducing agents: L. Horner, W.D. Balzer, Tetrahedron Lett. 17 (1965) 1157;
(b) H. Fritzsche, U. Hasserodt, F. Korte, G. Friese, K. Adrian, H.J. Arenz, Chem. Ber. 97 (1964) 1988;
(c) H. Fritzsche, U. Hasserodt, F. Korte, G. Friese, K. Adrian, Chem. Ber. 98 (1965) 171;
(d) K. Naumann, G. Zon, K. Mislow, J. Am. Chem. Soc. 91 (1969) 2788;
(e) K. Naumann, G. Zon, K. Mislow, J. Am. Chem. Soc. 91 (1969) 7012.
[43] L. Qiu, F.Y. Kwong, J. Wu, W.H. Lam, S. Chan, W.-Y. Yu, Y.-M. Li, R. Guo, Z. Zhou, A.S.C. Chan, J. Am. Chem. Soc. 128 (2006) 5955.
[44] W. Zhang, F. Zie, H. Yoshinaga, T. Kida, Y. Nakatsuji, I. Ikeda, Synletters 8 (2006) 1185.
[45] D. Liu, X. Zhang, Eur. J. Org. Chem. 4 (2005) 646.
[46] G.P.C.M. Dekker, A. Buljs, C.J. Elsevier, K. Vrieze, P.W.N.M. van Leeuwen, W.J.J. Smeets, A.L. Spek, Y.F. Wang, C.H. Stam, Organometallics 11 (1992) 1937.
[47] W.J. Marshall, V.V. Grushin, Organometallics 22 (2003) 555.
[48] R.J. Goodfellow, B.F. Taylor, J. Chem. Soc., Dalton Trans. 16 (1974) 1676.
[49] B.M. Still, P.G.A. Kumar, J.R. Aldrich-Wright, W.S. Price, Chem. Soc. Rev. 36 (2007) 665.
[50] P.S. Pregosin, Coord. Chem. Rev. 44 (1982) 247.
[51] S.O. Grim, R.L. Keiter, W. McFarlane, Inorg. Chem. 6 (1967) 1133.
[52] P.S. Pregosin, R.W. Kunz, ^{31}P and ^{13}C NMR of Transition Metal Phosphine Complexes, NMR 16 Basic Principles and Progress, P. Diehl, E. Fluck, R. Kosfeld (Eds.), Springer-Verlag, 1979.
[53] S. Favaro, L. Pandolfo, P. Traldi, Rapid Commun. Mass Spectrom. 11 (1997) 1859.
[54] W. Henderson, C. Evans, Inorg. Chim. Acta 294 (1999) 183.
[55] (a) S.L.G. Husheer, O. Forest, M. Henderson, J.S. McIndoe, Rapid Commun. Mass Spectrom. 19 (2005) 1352;
(b) P.J. Dyson, A.K. Hearley, B.F.G. Johnson, J.S. McIndoe, C. Whyte, P.R.R. Langridge-Smith, Rapid Commun. Mass Spectrom. 15 (2001) 895;
(c) P.J. Dyson, B.F.G. Johnson, J.S. McIndoe, P.R.R. Langridge-Smith, Rapid Commun. Mass Spectrom. 14 (2000) 311.
[56] C.P.G. Butcher, P.J. Dyson, B.F.G. Johnson, T. Khimyak, J.S. McIndoe, Chem. Eur. J. 9 (2003) 944–950.
[57] CSD database 5.29 for 17 structures consistent with Pt(P)(PO)R2 (where R was typically phosphine) mean distances were P–O–Pt 2.094 Å; P–Pt 2.222 Å.
[58] J.J. MacDougall, J.H. Nelson, Inorg. Nucl. Chem. Lett. 15 (1979) 315.
[59] J. Mason (Ed.), Multinuclear NMR, Plenum Press, New York, 1987, pp. 395–396.
[60] N.J. Goodwin, W. Henderson, B.K. Nicholson, Inorg. Chim. Acta 295 (1999) 18.
[61] The concentration of the phenyllithium solution was determined by double titration against standardized HCl$_{(aq)}$; the effective concentration (total basicity less residual basicity after treatment with 1,2-dibromoethane) was typically in the 0.6–0.9 mol L^{-1} range.
[62] M. Schlosser, Organometallics in Synthesis: A Manual, 2nd ed., Wiley, 2002.
[63] D. Drew, J.R. Doyle, Inorg. Synth. 28 (1990) 346.